Surveying the nuclear caloric curve

Y.G. Ma, A. Siwek, J. Peter, F. Gulminelli, R. Dayras, L. Nalpas, B. Tamain, E. Vient, G. Auger, Co. Bacri, et al.

BB

LPC CAEN

LABORATOIRE DE PHYSIQUE CORPUSCULAIRE

ISMRA - Boulevard Maréchal Juin - 14050 CAEN CEDEX - FRANCE

SURVEYING THE NUCLEAR CALORIC CURVE

Ma Y.-G. , A. Siwek, J. Péter, F. Gulminelli, R. Dayras, L. Nalpas, B. Tamain, E. Vient, G. Auger, Ch. O. Bacri, J. Benlliure, E. Bisquer, B. Borderie, R. Bougault, R. Brou, J. L. Charvet A. Chbihi , J. Colin, D. Cussol, E. De Filippo, A. Demeyer, D. Doré, D. Durand, P. Ecomard, P. Eudes, E. Gerlic, D. Gourio, D. Guinet, R. Laforest, P. Lautesse, J. L. Laville, L. Lebreton, J.F. Lecolley, A. Le Fèvre, T. Lefort, R. Legrain, O. Lopez, M. Louvel, J. Łukasik, N. Marie, V. Métivier, A. Ouatizerga, M. Parlog, E. Plagnol, A. Rahmani, T. Reposeur, M.F. Rivet, E. Rosato, F. Saint-Laurent, M. Squalli, J.C. Steckmeyer, M. Stern, L. Tassan-Got, C. Volant, J.P. Wieleczko

July 1996

LPCC 96-10

Submitted to Physics Letters B

INSTITUT NATIONAL
DE PHYSIQUE NUCLEAIRE ET DE PHYSIQUE DES PARTICULES

CENTRE NATIONAL DE LA RECHERCHE SCIENTIFIQUE

INSTITUT DES SCIENCES
DE LA MATIERE ET DU RAYONNEMENT

UNIVERSITÉ DE CAEN

Téléphone : 31 45 25 00
Télécopie : 31 45 25 49

Surveying the nuclear caloric curve. ⋆

Ma Y.-G. [a,1], A. Siwek. [a,2], J. Péter [a], F. Gulminelli [a], R. Dayras [b], L. Nalpas [b], B. Tamain [a], E. Vient [a], G. Auger [c], Ch.O. Bacri [d], J. Benlliure [c], E. Bisquer [e], B. Borderie [d], R. Bougault [a], R. Brou [a], J.L. Charvet [b], A. Chbihi [c], J. Colin [a], D. Cussol [a], E. De Filippo [b], A. Demeyer [e], D. Doré [d], D. Durand [a], P. Ecomard [c], P. Eudes [f], E. Gerlic [e], D. Gourio [f], D. Guinet [e], R. Laforest [a] P. Lautesse [e], J.L. Laville [f], L. Lebreton [e], J.F. Lecolley [a], A. Le Fèvre [c], T. Lefort [a], R. Legrain [b], O. Lopez [a], M. Louvel [a], J. Łukasik [d], N. Marie [c] V. Métivier [f], A. Ouatizerga [d], M. Parlog [d], E. Plagnol [d], A. Rahmani [f], T. Reposeur [f], M.F. Rivet [d], E. Rosato [a], F. Saint-Laurent [c], M. Squalli [d], J.C. Steckmeyer [a], M. Stern [e], L. Tassan-Got [d], C. Volant [b], J.P. Wieleczko [c]

[a] *LPC Caen (IN2P3-CNRS/ISMRA et Université), F-14050 Caen, France*

[b] *CEA DAPNIA-SPhN, CE Saclay, F-91191 Gif sur Yvette, France*

[c] *GANIL (DSM-CEA/IN2P3-CNRS), B.P.5027, F-14021 Caen, France*

[d] *IPN Orsay (IN2P3-CNRS), F-91406 Orsay, France*

[e] *IPN Lyon (IN2P3-CNRS/Université), F-69622 Villeurbanne, France*

[f] *SUBATECH (IN2P3-CNRS/Université), F-44072 Nantes 03, France*

Abstract

The 4π array INDRA was used to detect nearly all charged products emitted in Ar+Ni collisions between 52 and 95 MeV/u. The charge, mass and excitation energy E^* of the quasi-projectiles have been reconstructed event by event. Excitation energies up to 25 MeV per nucleon are reached. Apparent temperatures obtained from several double isotopic yield ratios Tr^0 show different dependences upon E^*. $T^0_{^6Li-^7Li-^3He\alpha}$ yields the highest values, as well as the high energy slopes Ts of the kinetic energy spectra. Two statistical models, sequential evaporation and gas in complete equilibrium, taking into account side feeding and discrete excited states population, show that the data can be explained by a steady increase of the initial temperature with excitation energy without evidence for a liquid-gas phase transition.

The dependence of nuclear temperature upon excitation energy has been experimentally studied with increasing values of excitation energy over the years. At excitation energies per nucleon, E^*/A, lower than 6 MeV the temperatures Ts deduced from the kinetic properties of the emitted particles and clusters (slope parameter of the Maxwell-Boltzmann distributions of kinetic energies) follow the Fermi gas law : $E^* = A/k\ T^2$. The value of the inverse level density parameter k was found to be in the range 8 to 13[1]. When excitation energies up to 10 MeV per nucleon were reached, temperatures obtained from the relative populations of excited levels in the emitted light nuclei did not overcome 5-6 MeV [2], but this limitation could be explained by side-feeding effects. Such hot nuclei were formed in fusion or deep inelastic reactions. At incident energies above 40-50 MeV/u, binary dissipative collisions dominate and the quasi-projectiles reach excitation energies per nucleon and kinetic temperatures above 10 MeV[3,4]. The study of projectile "spectators" in reactions at several hundreds of MeV/u allowed one to reach higher excitation energies [5]. In this Aladin experiment, the temperature was obtained via the relative abundances of two isotope pairs [6]. The relation between this temperature Tr^0 and E^*/A was interpreted as indicating a phase transition, with the nuclear gas regime dominating above $E^*/A = 10$ MeV, as predicted [7]. Very recently, a monotonic increase of the temperature with excitation energy was observed [8,9]. Some questions were raised about the significance of these caloric curves [10–13], about the role played by the mass dependence of the decaying nucleus upon E^*/A in the Aladin experiment[14], as well as the strong effects of side-feeding, especially at high temperatures [15].

This letter reports on a study of the temperature-excitation energy relationship for E^* ranging from 2 to 24 MeV per nucleon in the quasi-projectile issued from the reaction $^{36}Ar + ^{58}Ni$ at 52, 74 and 95 MeV/u. In comparison to the Aladin experiment, the mass of the decaying nucleus is smaller but it is nearly independent of excitation energy. Moreover, different prescriptions for the determination of temperatures were applied and compared with each other. These comprised the apparent temperatures extracted from several pairs of isotopes and from the slopes of light charged particle kinetic energy spectra. In contrast to [5] and in agreement with [9], no indication was found for a phase transition.

The kinetic energies of charged products were measured with the 4π detector array INDRA covering 90% of the 4π solid angle [16]. Isotopic separation was achieved for elements up to Z=4. Above, the mass was taken on the β-stability line. In some events (mostly peripheral and semi-peripheral collisions) a large projectile fragment may be emitted into the beam pipe ($\theta \leq 2^0$) or in an insensitive area. This would lead to an erroneous reconstruction of the quasi-projectile. Such events were discarded by requiring that the total parallel momentum of all detected products be larger than 80% of the projectile momentum. In order to sort the events according to the violence of the collision, the sum of transverse momenta of Z=1 and 2 particles was used. The measured reaction cross section was

---

* Experiment performed at Ganil

[1] on leave of absence from Institute of Nuclear Research, Shanghai, China.

[2] on leave of absence from Instytut Fizyki Jadrowej, Cracow, Poland.

divided in 20 impact parameter bins, each corresponding to $\simeq$50 mb (6 bins of central collisions) or $\simeq$100 mb (other bins).

As for heavier and lighter systems having the same mass asymmetry studied previously at neighbouring incident energies [3,4], the dominant process is the formation of a quasi-projectile (QP) and a quasi-target (QT) accompanied by dynamical (also called pre-equilibrium) emission centered around mid-rapidity. The same conclusion was reached for nearby symmetric systems [17]. Part of the QT products were undetected or could not be identified in charge, but all QP products have velocities well above the detection and isotopic separation thresholds. Therefore, only the QP was reconstructed as in [4]. Its velocity was obtained as the center-of-gravity of momenta of fragments with masses $\geq$3 and rapidities above mid-rapidity, through an iterative process.

Determining a temperature value is justified only if thermal equilibrium was achieved in the source. Experimentally one can check that the angular distributions of various products are isotropic in the source frame (or forward-backward symmetric if the source has a large spin). This is not sufficient to establish that equilibrium had been attained, but this is a necessary condition. We selected the products, ranging from protons to ^{8}Li, attributed to the QP and examined their angular distributions in the QP frame. The mid-rapidity contribution is clearly seen near 180^{o} , eventhough it is not large. These distributions are nearly flat below 90^{o} and can be attributed to de-excitation of a likely equilibrated nucleus. Thermal equilibrium was also established for vaporization events [18], i.e. at high excitation energies . A crucial test of thermalisation of the decaying nucleus is an agreement between the initial temperature values obtained by various methods [13]. Therefore we will determine several temperatures and compare them.

The forward hemisphere (in QP frame) can be used to determine the QP excitation energy and temperature values. The QP charge was reconstructed by taking its heaviest product and twice the other products located in the forward hemisphere [3,4,17]. This minimizes the mid-rapidity contribution. The primary mass was obtained assuming conservation of the N/Z ratio of the system. The number of neutrons emitted by the QP was estimated from the difference between this mass and the sum of masses of the charged products. The average mass was found to be slightly below the projectile mass and decreasing by $\simeq$ 15% from peripheral to violent collisions. In order to study nuclei with defined masses, QP's with $A = 34 \pm 20$ % were kept for further analysis.

The QP excitation energy is equal to the mass balance between the QP mass and its products, added to the sum of kinetic energies of its products in its frame. The kinetic energy of neutrons was taken as the average kinetic energy of protons in the same impact parameter bin, minus 2 MeV to take into account the absence of the Coulomb barrier. Due to large fluctuations in the energy sharing between QP and QT, the excitation energy per nucleon reaches values above the available energy per nucleon in central collisions, as already seen for this system [18].

Since the results are sensitive to the velocity, charge and mass of the QP, we used two other reconstruction methods. In the method based on the "thrust" variable [19] the velocities and charges of the QP and QT were determined simultaneously, so it required to use almost complete events ($\geq 80\%$ of the total charge), which eliminated peripheral collisions, and it was sensitive to the detection thresholds. The method based on the "minimum spanning tree" [20] was not subject to such limitations [21]. These two methods yielded results similar to those obtained with the first method. The corresponding uncertainties are taken into account in the error bars in fig. 2 and 3.

Temperatures were calculated from the yields Y of several pairs of light isotopes differing by one neutron, according to [6]:

$$Tr^0_{n-d} = B/\ln(a.\frac{(Y(Z_n,A_n)/Y(Z_n,A_n+1)}{(Y(Z_d,A_d)/Y(Z_d,A_d+1)} \quad (1)$$

where ***n (d)*** stands for the pair of isotopes with the smallest (largest) binding energy difference, and appears at the numerator (denominator) on the right side. B is the difference of binding energy differences. The larger the value of B, the higher the range of temperatures where this formula gives accurate values. a depends on the spins of the populated states : ground states and excited states[6]. By choosing isotopes which do not have low energy levels decaying via γ emission, one can calculate a with the ground states only, as in [5]. This approximation is indicated by the index 0. But at high temperatures, high energy levels contain a significant part of the yield, especially when they have a large spin. When they decay via γ emission, they contribute to the yields in eq. 1. Another problem is that several levels decay via particle emission. This reduces the yields of the decaying fragments and increases the yields of daughter fragments (side-feeding) [15]. Therefore Tr^0 is only an apparent temperature.

Let us examine the Tr^0 values obtained at 95 MeV/u with various isotope pairs listed in the caption of fig. 1. Solid symbols correspond to the impact parameter sorting described above. For each point the abscissa is the average excitation energy per nucleon. Since for each bin the excitation energy distribution is broad, one may worry about the validity of the sorting. To answer this question, open symbols show E^*/A values obtained event by event without neither sorting nor averaging. Each point corresponds to a different cross section; the one at the highest E^*/A value corresponds to $\approx$ 7mb. They quite agree with the solid symbols.

The large differences between Tr^0 values obtained from different isotope pairs confirm that these apparent temperatures cannot be used as a measure of the initial temperature.

When B is not large ($\approx$ 5 MeV), i.e. p,d-^{6}Li,^{7}Li and ^{7}Li,^{8}Li-^{6}Li,^{7}Li, the curves increase very slowly with E^*/A and saturate at low Tr^0 values. Such ratios are useless. When the isotopes having the largest binding energy difference, $^3He - \alpha$, are involved, larger B values are obtained (13 to 18 MeV) and Tr^0 increase more with E^*/A. The values of

Tr^0 obtained with the isotopes $p-d$ and $d-t$ at the numerator never exceed 6 MeV. $T^0_{^6Li^7Li-^3He\alpha}$ reaches higher values, which may mean it kept a better memory of the initial temperatures. It was used in the Aladin experiment[5]. Up to $\simeq$10 MeV per nucleon it increases monotonously and no plateau is observed, at variance with the Aladin data. The T^0_r values seem to be close to those shown in [5], but in the present work the value of B was taken according to [6] whereas in [5] B (and Tr^0) was increased by 20%. If this increase is not taken into account, our values are $\simeq$ 25% higher. This may be related to the lighter system studied here [14]. Above E*/A=10 MeV, the slope increases slightly.

Some QP's are vaporized in light particles (p to α [18]). Their $T^0_{pd-^3He\,\alpha}$ and $T^0_{dt-^3He\,\alpha}$ values are displayed in fig. 1b, together with values obtained when also the QT's are vaporized [18] . They are the same as in fig. 1a. This indicates that fluctuations in the partition of usual QP's produced such events [18]. When the particle range includes Li nuclei,$T^0_{^6Li^7Li-^3He\alpha}$ is also the same as for all events at high excitation energies since the heaviest fragments there are usually Li or He. A difference appears progressively at lower excitation energies since the proportion of events having heavier fragments increases.

It must be noted that experimental uncertainties affect the shape of such curves, since the sensitivity of the logarithmic function in eq. (1) increases rapidly with T. For $T^0_{^6Li^7Li-^3He\alpha}$, when the real temperature is 5 MeV, an error of +20% on the double ratio leads to a shift of -6% on Tr^0. At 10 and 15 MeV, the shift becomes -12% and -17% respectively. An error of -20% leads to respective shifts of +9%, +20% and +34%. If the double ratio value is overestimated (underestimated) by a constant percentage at all excitation energies, the curve is tilted downwards (upwards). If the percentage and/or sign varies with E^*/A, the distortion is worse. This effect may be responsible for the difference between the Aladin data and the present data.

Alternative information is contained in the kinetic energy spectra. The slope parameters Ts were obtained via the usual fits with Maxwell-Boltzmann distributions for light particles (less sensitive to possible collective expansion) and are shown in fig. 1c. They are also apparent temperatures, averaged over the de-excitation chain and affected by successive recoil effects. They agree together within $\pm$ 10 % and increase rapidly with E^*/A.

Since low values of excitation energies are reached in peripheral collisions and high values in central collisions, different collision dynamics at different impact parameters could possibly contribute to the observed behavior. Data obtained at 52 and 74 MeV/u were analyzed with the same method after removing the larger part of the few fusion events present at 52 MeV/u. At the same excitation energy value obtained at different impact parameters at the three energies, the three Tr^0 and Ts values agree with each other. This means that there is no large impact parameter effect and that the decay of the QP is dictated by its excitation energy [4,18,22].

One must check whether the various apparent temperatures can be reproduced with the

same initial temperature in calculations including the population of all excited states contributing to the reduction or the feeding of the isotopes of interest. We have modelled the de-excitation of the quasi- projectile in the framework of two simple statistical models. Sequential decay is known to occur at low excitation energy. while a rapid decay - almost simultaneous - is likely at the highest excitation energies. We have then considered these two cases. The population of discrete excited states of emitted fragments was taken into account and their decay was followed until they reached a state which did not decay via particle emission; the final distributions were then corrected for the sidefeeding of resonance decay [25]. All the known nuclear species were included up to an atomic number Z=16 corresponding to the average source charge, with the corresponding discrete levels which are characterized by a width smaller than a cutoff value Γ_0 [23]. The value of Γ_0 is related to the minimum lifetime τ assumed for the decaying source ($\tau \geq \hbar/\Gamma_0 \approx 200$ fm/c for the smaller Γ_0= 1 MeV here considered).

In the first model, the standard evaporation theory was applied by considering sequential emission of particles and fragments [25]. he resulting events were filtered through the detector acceptance and analyzed like the experimental data. Two different correlations between initial temperature and excitation energy were studied, as shown in the top left panel in fig. 2 : i) a monotonic increase (Fermi gas), ii) a plateau between 3.6 and 11 MeV per nucleon followed by a rise above 11 (simulating a phase transition, as suggested in [7]).

The resulting apparent temperatures are plotted in the other panels in fig. 2 and compared to the data. The vertical size of solid symbols indicates the experimental uncertainty (range of values obtained via different methods and corrections). The calculated temperatures are sensitive to Γ_0 above 12 MeV per nucleon. Let us note that the effect of including or not broad levels is more easily understood by looking at the yields of individual isotopes . Some of them vary monotonically with Γ_0; others increase and decrease with Γ_0, due to the competition between feeding from heavier isotopes and their own particle decay. Fig. 2 was made with Γ_0= 1.5 MeV.

The results of the calculation with a plateau clearly disagree with most data. The Fermi gas results exhibit a good agreement for $T^0_{pd-^3He\alpha}$, $T^0_{pd-^6Li^7Li}$ and Ts for p's and d's . These results are not very sensitive to the value of the inverse level density parameter k. A disagreement remains for $T^0_{^6Li^7Li-^3He\alpha}$ above 12 MeV per nucleon. The reason is the yield of ^{3}He is underestimated and the α yield is overestimated after side-feeding is taken into account, whatever the value of Γ_0. Anyway at high excitation energies the second model is expected to be more realistic.

In the second set of calculations (*CEM* model, see ref. [18]), the emitting source is viewed as a nuclear gas in thermal and also chemical equilibrium undergoing simultaneous multifragmentation at a given density ρ and temperature T [24]. The density populations of the different nuclear species are uniquely determined from conservation laws and the

equilibrium distributions in the macrocanonical ensemble

$$n_i = \frac{g_i(m_i T)^{3/2}}{\sqrt{2}\pi^2\hbar^3} \int_0^\infty dz\sqrt{z}\Big(exp(z - \frac{\mu_i}{Tini} + \frac{E_i}{Tini}) \pm 1\Big)^{-1} \tag{2}$$

where m_i is the mass of the fragment, g_i the degeneracy factor, E_i its intrinsic energy (ground state energy plus excitation energy), the sign + (−) accounts for Fermi (Bose) statistics, and the mass action law of chemical equilibrium allows to determine the chemical potential of the i-th species as a function of the two constant chemical potentials for neutrons and protons μ_n, μ_p, which are determined at any given density to ensure conservation of the total neutron and proton number. Corrections to the ideal gas are also included in the form of excluded volume effects [26]. The excitation energy has been calculated as the total energy of the freeze out configuration with respect to the binding energy of the source, and the interparticle electrostatic interaction has been approximately accounted for by means of an average Coulomb field calculated at the proper freeze out density. This latter quantity has been fixed to reproduce the experimental excitation energy dependence of the measured ratio between proton and alpha yields. It turns out that the correlation between the chemical potential and the proton over alpha ratio is very strong, therefore each excitation energy bin can be associated with a unique couple of T, μ_n parameters. The proton chemical potential is fixed by the hypothesis of an isospin symmetric $N/Z = 1$ source, and we have verified that an isospin asymmetry $N/Z = 1.2$ modifies the apparent temperatures calculated within the experimental error bars.

In fig. 3 top we show the calculated Tr^0 values and the Ts parameter for deuterons as a function of excitation energy, compared to the data of fig. 1. The slope change around E^*/A=10 MeV is due to the fact that the excitation energy is dominated by the reaction Q-value at low temperature, and at high temperature by the average kinetic energy of the fragments. As one may expect, at low excitation energy the model fails completely to reproduce the data: the hypothesis of a sudden multifragmentation is clearly inadequate to describe the low energy evaporative regime. On the other side, for excitation energies greater than $\approx$ 10 MeV per nucleon, the data are fairly well reproduced and all the different caloric curves seem compatible with the scenario of a gas of non interacting nuclear species in thermodynamical equilibrium. The temperature used in the calculation ranges from 2 to 18 MeV, and its value at each excitation energy is practically indistinguishable from the value of Ts. As a matter of fact, the deuteron yield is not much augmented by resonance decay (only 4% of the deuterons come from a resonance decay at E^*/A=20 MeV) and the secondary deuterons modify only the low energy part of the spectrum. The Tr^0 values do not depend strongly on the freeze out density used: at E^*/A=20 MeV a 45% variation of the density induces a 30% variation of the proton-over-alpha ratio and only a 3% variation of Tr^0.

These results were obtained with Γ_0=2 MeV. The sensitivity to this parameter is shown in fig. 3 bottom, which displays three different calculations of the apparent temperatures Ts

from deuterons and $T^0_{^6Li^7Li-^3He\alpha}$. As one may expect, $T^0_{^6Li^7Li-^3He\alpha}$ increases by decreasing Γ_0, i.e. decreasing the overall contribution of sidefeeding. This is true also for the other Tr^0's not shown in the figure. The difference between the various temperature parameters is essentially due to sidefeeding. However, for a source lifetime $\tau \leq 100$ fm/c ($\Gamma_0 \geq 2$) the results are not strongly dependent on the number of resonances included.

In conclusion, apparent temperatures obtained from isotope ratios and kinetic energy distributions were determined for quasi-projectiles formed in collisions of ^{36}Ar on Ni at 95, 74 and 52 MeV/u. The QP masses are nearly constant over the whole range of excitation energies which reaches 24 MeV per nucleon. Two types of calculations show that isotope apparent temperatures are very sensitive to the role of high energy resonances and the determination of initial temperatures is subject to a large uncertainty. At excitation energies above 10 MeV per nucleon, isotope ratios give apparent temperatures much lower than the initial temperatures. Values obtained with the double pair ^{6}Li^{7}Li-^{3}Heα are more realistic than those obtained with other isotope ratios. The kinetic temperatures (slope parameters) of light particles keep a good memory of the initial temperature. No evidence is found for a plateau followed by a rise (first order liquid-gas phase transition) in the relationship between T and E^*/A, neither in the experimental data (apparent temperatures), nor in the initial temperatures obtained via calculations. The temperature increases steadily with excitation energy on the whole range of excitation energies. Up to $\approx$10 MeV per nucleon, the relationship between T and E^*/A is very close to that of a Fermi gas and sequential statistical decay can explain the data. At higher excitation energies, multifragmentation sets in and the temperature increases slightly faster with excitation energy. Instead of a rather sharp transition, a gradual evolution is observed.

One of us (M.Y.G.) wants to thank the CNRS - K.C. WONG Foundation for a grant. M.Y.G. and A.S. thank LPC Caen for its hospitality.

References

[1] D. Fabris et al., Phys. Lett. B **196** (1987) 429.
K. Hagel et al., Nuc. Phys. **A486** (1988) 429.
R. Wada et al., Phys. Rev. **C 39** (1989) 497.

[2] J. Pochodzalla et al., Phys. Rev. **C 35** (1987) 1695 and references therein.

[3] A. Kerambrun et al., Report LPC Caen 94-14 (1994), unpublished.
J.C. Steckmeyer et al., Phys.Rev. Lett. **76** (1996) 4895.

[4] J. Péter et al., Nucl. Phys. **A593** (1995) 95.

[5] J. Pochodzalla et al., Phys. Rev. Lett. **75** (1995) 1040.

[6] S. Albergo et al, Nuovo Cimento **A89** (1985) 1.

[7] J. Bondorf et al, Nucl. Phys. **A443** (1985) 321, **A444** (1985) 460, **A448** (1986) 753.

[8] M. Morjean et al., Nucl.Phys. **A591** (1995) 371.

[9] J. A. Hauger et al., Phys. Rev Lett. 77 (1996) 235.

[10] D. H. E. Gross et al., Phys. Lett. B 200 (1988) 397.

[11] Sa B.-H., Nucl. Phys. **A499** (1989) 480.

[12] L. G. Moretto et al., Phys. Rev. Lett. **76** (1996) 2822.

[13] X. Campi et al., preprint IPN Orsay IPNO TH 96-17 (1996), submitted to Phys. Rev. C.

[14] J. Natowitz et al., Phys. Rev. C **52** (1995) R2322.

[15] M. B. Tsang et al., Phys. Rev. C **53** (1996) R1057.

[16] J. Pouthas et al., Nucl. Inst. and Meth.**A357** (1995) 418, **A369** (1996) 222.

[17] V. Métivier et al., Proc. XXXIIIrd Int. Winter Meeting on Nucl. Phys., Bormio (Italy), January 1995, ed. by I. Iori.

[18] B. Borderie et al., submitted to Phys. Lett. B

[19] J. Cugnon and D. L'Hôte, Nucl. Phys. **A387** (1983) 519.

[20] C.T. Zahn, IEEE Trans. Comp. **C20** (1971) 68.

[21] L. Nalpas, Ph. D. thesis, in preparation.

[22] C. A. Ogilvie et al, Phys. Rev. Lett **67** (1991) 1214.

[23] Table kindly communicated by J. Konopka and H. Stöcker and completed with the widths taken in : F. Ajzenberg-Selove Nucl. Phys. **A320**(1979)1-**A449**(1986)1-**A475**(1987)1-**A506**(1990)1, D. R. Tilley et al. Nucl. Phys. **A564**(1993)1, P. M. Endt Nucl.Phys. **A521**(1990)1.

[24] A.Z. Mekjan, Phys. Rev. C **17** (1978) 1051

[25] D. Durand et al , *in preparation*

[26] R. K. Tripathi and L.W. Townsend Phys. Rev. C **50** (1994) R7.

Figure captions

Fig 1: Measured apparent temperatures versus excitation energy per nucleon of the quasi-projectile formed in ^{36}Ar collisions on ^{58}Ni at 95 AMeV.
a : Isotope temperatures. Solid symbols : average excitation energy obtained by sorting events according to the violence of the collision (see text). Open symbols : excitation energy obtained event by event.
Circles : isotope pairs ^{6}Li,^{7}Li - ^{3}He,α
Stars : d,t-^{3}He,α
Squares : p,d - ^{3}He,α
Crosses : ^{7}Li,^{8}Li - ^{6}Li,^{7}Li
Triangles : p,d - ^{6}Li,^{7}Li
For orientation, the Fermi gas relation is shown with A/12 (dot-dashed line) and A/8 (dotted line).
b : Same symbols as above.
Circles : results obtained for QP's with $Z_{heaviest\ QP\ product} \leq 3$. Other open symbols : for vaporized QP's ($A_{heaviest\ QP\ product} \leq 4$). Solid symbols : when both the QT's and QP's vaporized.
c : Slope parameters from kinetic energy spectra for protons (circles), deuterons (squares), tritons (triangles), ^{3}He (crosses) and α-particles (stars).
For clarity, error bars show statistical uncertainties only.

Fig 2 : Top left panel : correlation between initial temperature $Tini$ and excitation energy per nucleon E^*/A assumed in statistical decay calculations.
Other panels : dependence of the apparent temperature on E^*/A. Dots : experimental data. Solid lines : Fermi gas with level density parameter A/10. Dashed lines : liquid-gas phase transition. From top to bottom : apparent temperatures from double isotope ratios ^{6}Li,^{7}Li - ^{3}He,α, p,d - ^{3}He,α and d,t-^{3}He,α, and slope parameters from proton and deuteron kinetic energy spectra.

Fig 3. Top panel: Correlation between apparent temperatures and excitation energy obtained via a multifragmentation calculation and compared to data. Solid symbols : experimental data. Upper triangles : Ts for deuterons (fig. 1c). Other symbols : T_r^0 for the same isotope pairs as in fig. 1a. Lines and open symbols : calculated values corresponding to the closed symbol with the same shape. Bottom panel: influence of the maximum width of discrete levels on the kinetic temperature Ts from deuterons and on the isotope temperature $T^0_{6Li^7Li-^3He\alpha}$. For orientation, the dashed-dotted line shows $E* = A/10 * T^2$.

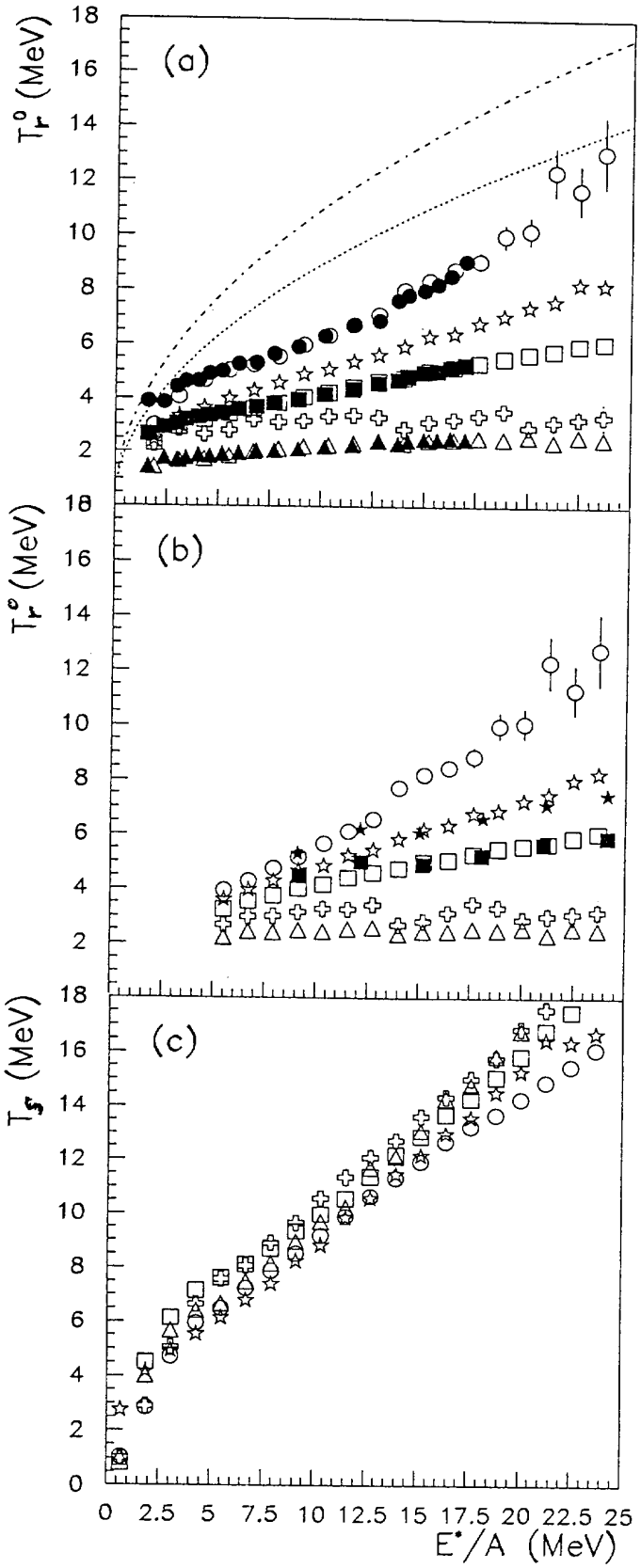
(a)
(b)
(c)
T_{p}^{0} (MeV)
T_{p}^{0} (MeV)
T_{γ} (MeV)
E*/A (MeV)
0 2.5 5 7.5 10 12.5 15 17.5 20 22.5 25

Fig 1

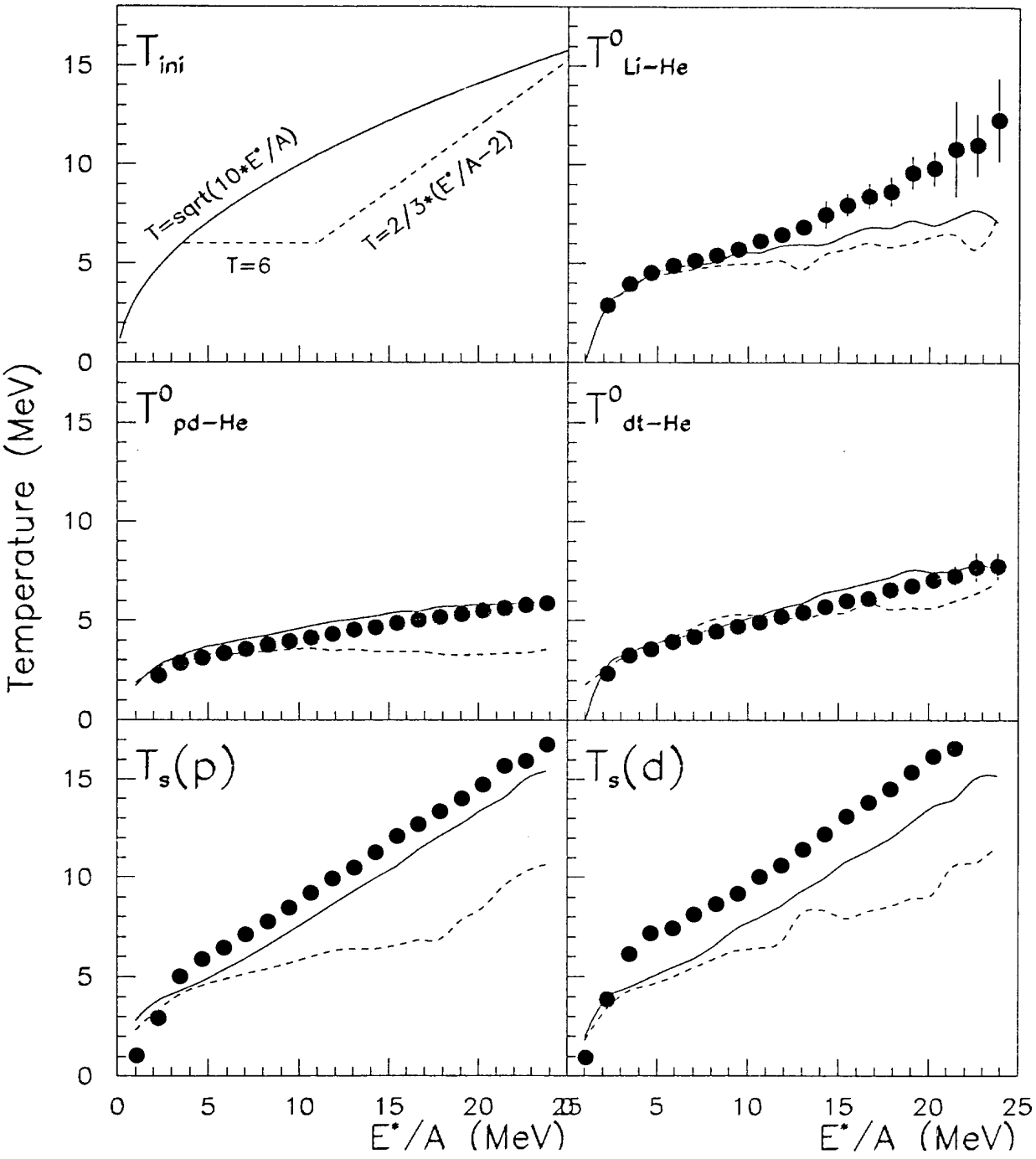
T_{ini}
T=sqrt(10*E*/A)
T=6
T=2/3*(E*/A-2)
T^0_{Li-He}
T^0_{pd-He}
T^0_{dt-He}
$T_s(p)$
$T_s(d)$
Temperature (MeV)
E*/A (MeV)
E*/A (MeV)
0
5
10
15
20
25

Fig 2

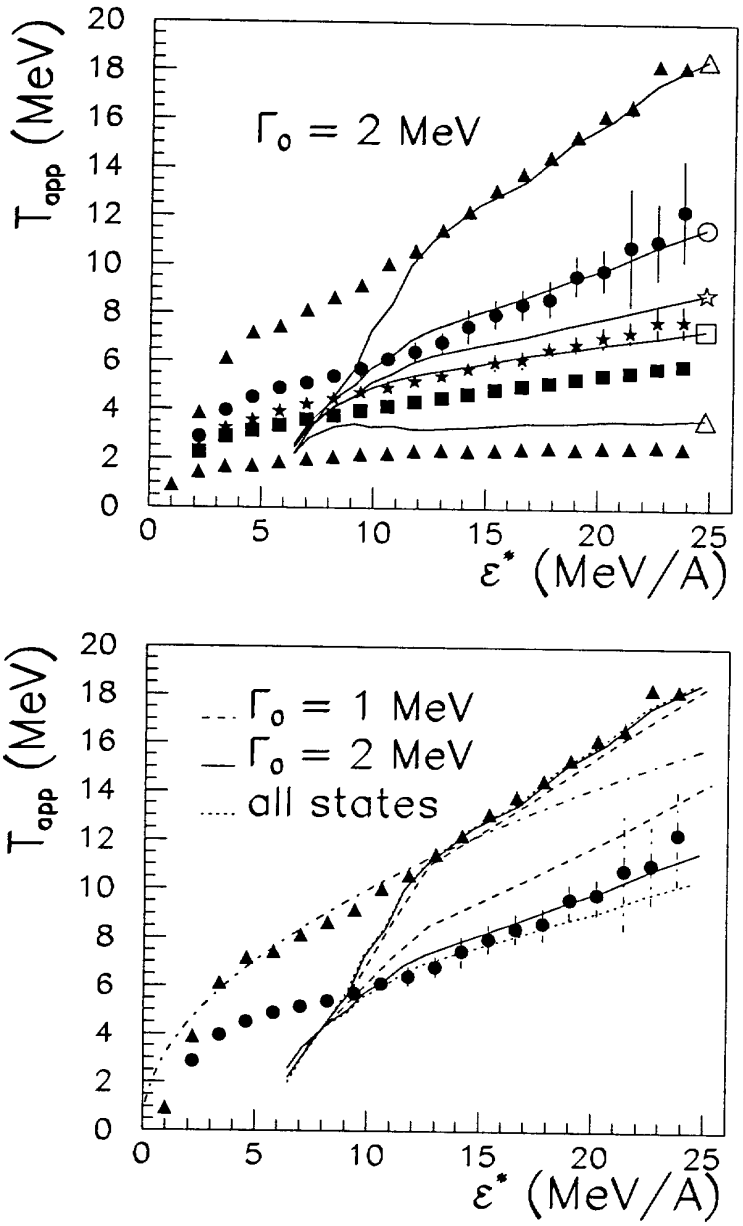
T_{app} (MeV)
Γ_0 = 2 MeV
ε^* (MeV/A)
T_{app} (MeV)
Γ_0 = 1 MeV
Γ_0 = 2 MeV
all states
ε^* (MeV/A)

Fig. 3